Quantum oscillations in the kinetic energy density: Gradient corrections from the Airy gas

A. Lindmaa,[1,*] A. E. Mattsson,[2,†] and R. Armiento[1,‡]

[1]*Department of Physics, Chemistry and Biology (IFM), Linköping University, SE-581 83 Linköping, Sweden*

[2]*Multi-Scale Science MS 1322, Sandia National Laboratories, Albuquerque, New Mexico 87185-1322, USA*

(Received 4 March 2014; revised manuscript received 16 June 2014; published 22 August 2014)

We derive a closed-form expression for the quantum corrections to the kinetic energy density in the Thomas-Fermi limit of a linear potential model system in three dimensions (the Airy gas). The universality of the expression is tested numerically in a number of three-dimensional model systems: (i) jellium surfaces, (ii) confinement in a hydrogenlike potential (the Bohr atom), (iii) particles confined by a harmonic potential in one and (iv) all three dimensions, and (v) a system with a cosine potential (the Mathieu gas). Our results confirm that the usual gradient expansion of extended Thomas-Fermi theory does not describe the quantum oscillations for systems that incorporate surface regions where the electron density drops off to zero. We find that the correction derived from the Airy gas is universally applicable to relevant spatial regions of systems of types (i), (ii), and (iv), but somewhat surprisingly not (iii). We discuss possible implications of our findings to the development of functionals for the kinetic energy density.

DOI: 10.1103/PhysRevB.90.075139 PACS number(s): 71.15.Mb, 31.15.E−, 05.30.Fk, 71.10.−w

I. INTRODUCTION

Since the early days of quantum mechanics, there has been an interest in accurately describing the kinetic energy (KE) of a system of noninteracting fermions given the particle density. Such descriptions have been paramount in the development of schemes for computations of physical properties of atoms, molecules, and solids which are in ubiquitous use today across disciplines. An exact treatment of the KE is provided by density functional theory (DFT) [1] à la Kohn-Sham (KS) [2], but the derivation and evaluation of approximate expressions of the kinetic energy is still an active area of research with applications in, e.g., orbital-free DFT (OF-DFT) [3–7], high-temperature applications of DFT, and as an intermediate step in developing improved approximations for the exchange-correlation energy. Applications are also found in the field of nuclear DFT [8] and trapped degenerate fermion gases [9].

A common starting point for most approximations of the KE is Thomas-Fermi (TF) theory [10,11], which is exact for a uniform electron gas. A number of historically important works have derived corrections to TF for a weakly inhomogeneous electron system as an expansion in gradients of the electron density [1,12–15], and we will refer to this as the extended TF (ETF) gradient expansion (GE). However, it has also been noted that for systems with surface regions, i.e., regions where the electron density drops to zero, the ETF GE of the kinetic energy density is not valid and further corrections of the same order in the density and density gradient are necessary (see, e.g., Refs. [16] and [17] and references therein for an extended discussion). Despite a frequent appeal to TF and ETF theory in the literature, the need for such corrections is rarely discussed.

In the present paper, we utilize a closed-form expression of the noninteracting KE of the Airy gas (AG) surface model system [18] to derive a modified ETF GE that includes the quantum corrections. When applying the obtained expression to other model systems with electron surfaces, e.g., the jellium surface model, or particles confined by hydrogenlike or harmonic potentials, we find these quantum corrections to provide a crucial correction to the local description of the kinetic energy density (KED). However, for two other systems that we investigate, i.e., a system with a cosine potential and a system confined by a harmonic potential in only one dimension, we find that neither of the two expansions holds unreservedly.

As was mentioned above, a prime reason for our interest in an accurate description of the KED of noninteracting fermions is the application of such a description in OF-DFT. The search for improved approximations of the KE has a long history in this field [3–5]. A few notable recent developments of generic KE approximations follows. Perdew and Constantin [6] have constructed a set of Laplacian-level density functionals based on an interpolation between the fourth-order GE and the von Weizsäcker, which give good results for, e.g., jellium surfaces and the AG. Lee *et al.* [7] extract coefficients for a GE expansion from neutral atoms in the limit of large atomic numbers Z and discuss the implications for coefficients in a generalized-gradient-type approximation. More sophisticated expressions are also being developed, e.g., approximations with density-dependent kernels from linear-response theory [5]. The present paper differs from these and other recent contributions in the field of OF-DFT in that the central result is not intended as a generalized approximation for the total KE. The focus in this work is instead to extract and study the formally exact behavior of the kinetic energy *density* in the limit of slowly varying densities in a system where a surface region is present. Exact limits such as this have historically been very important in the development of general approximations.

The rest of the paper is organized as follows: in Sec. II, we summarize the important equations for the kinetic energy, the class of edge electron gas model systems, and the Airy gas model. In Sec. III, we derive the central expression of this work: a gradient expansion of the kinetic energy density which includes the quantum corrections stemming from the Airy gas surface. In Sec. IV, we investigate the universality

*alexander.lindmaa@liu.se
†aematts@sandia.gov
‡rickard.armiento@liu.se

of the obtained expressions in a range of numerical tests. In Sec. V, we discuss our findings. Finally, Sec. VI presents a summary and our main conclusions.

II. BACKGROUND

Our primary interest in the KE of noninteracting fermions is due to its central importance in KS-DFT [2], and thus we will adopt the relevant terminology from this field. Hence, consider a system of N noninteracting fermions with ground-state particle density $n(\mathbf{r})$ which we assume to be continuous everywhere. The KE is given exactly in Hartree atomic units by the functional

$$T_\mathrm{s}[n] = -\frac{1}{2}\sum_{\nu:\epsilon_\nu\leqslant\mu}\int d^3r\,\psi_\nu^*(\boldsymbol{r})\nabla^2\psi_\nu(\boldsymbol{r}), \tag{1}$$

where ν labels available states including the spin degree of freedom, μ is the self-consistent chemical potential, and $\{\psi_\nu\}_{\nu=1}^{\infty}$ are the KS orbitals with corresponding eigenvalues $\{\epsilon_\nu\}_{\nu=1}^{\infty}$. The KS orbitals are formally functionals of $n(\boldsymbol{r})$, making Eq. (1) an implicit functional. Equation (1) directly defines one possible kinetic energy density (KED) as

$$\tau_1(\boldsymbol{r}) = -\frac{1}{2}\sum_{\nu:\epsilon_\nu\leqslant\mu}\psi_\nu^*(\boldsymbol{r})\nabla^2\psi_\nu(\boldsymbol{r}). \tag{2}$$

The KED is only unique up to a term that integrates to zero over the system in Eq. (1). In a closed or periodic system, Gauss' divergence theorem applied to ∇n gives that the Laplacian of the electron density $\nabla^2 n$ integrates to zero. This can be exploited to construct the following alternative KED, which is positive at all points in space:

$$\tau(\boldsymbol{r}) = \tau_1(\boldsymbol{r}) + \frac{1}{4}\nabla^2 n(\boldsymbol{r}) = \frac{1}{2}\sum_{\nu:\epsilon_\nu\leqslant\mu}|\nabla\psi_\nu(\boldsymbol{r})|^2. \tag{3}$$

This choice of KED is advantageous for developing approximations, since an approximation that fulfills the constraint $\tau(\boldsymbol{r})\geqslant 0$ will avoid the unphysical result $T_\mathrm{s}<0$ for all $n(\boldsymbol{r})$. We stress that Eq. (3) is taken as a definition, which makes τ valid without ambiguity even for open nonperiodic systems. However, the caveat for such systems is that τ is then not strictly a KED, since integration will not give T_s [one would instead need to integrate $\tau(\boldsymbol{r})-(1/4)\nabla^2 n(\boldsymbol{r})$].

A starting point for many approximations of τ is the TF approximation,

$$\tau^\mathrm{TF}[n] = C_\mathrm{TF}n^{5/3}(\boldsymbol{r}), \tag{4}$$

with $C_\mathrm{TF}=(3/10)(3\pi^2)^{2/3}$. Based on the scaling relation of the total noninteracting kinetic energy [19], one can assume τ to be homogeneous of degree 5/3 under uniform coordinate scaling [20]. Hence, a (semi)local density-functional approximation (DFA) of the KED takes the form

$$\tau^\mathrm{DFA}[n] = \tau^\mathrm{TF}[n]F_\tau^\mathrm{DFA}(s,q,\ldots), \tag{5}$$

where F_τ^DFA is the refinement factor, and the scaled gradient s and Laplacian q are

$$s = \frac{|\nabla n(\boldsymbol{r})|}{2(3\pi^2)^{1/3}n^{4/3}(\boldsymbol{r})}, \tag{6}$$

$$q = \frac{\nabla^2 n(\boldsymbol{r})}{4(3\pi^2)^{2/3}n^{5/3}(\boldsymbol{r})}. \tag{7}$$

We define as a *limit of slowly varying density* any limit where s,q and all higher-order terms $\to 0$.

Early efforts to find improved approximations of τ date back to 1935, when von Weizsäcker [21] derived a KED approximation with $F_\tau^\mathrm{vW}=(5/3)s^2$. Kirzhnits [12,13] used commutator operator formalism to derive gradient corrections to TF theory in the limit of a weakly perturbed uniform electron gas. A number of extensions to the original result have followed. Hohenberg and Kohn [1] developed a density gradient technique based on linear-response formalism. An expansion in $\hbar$ of the Green's-function representation due to Wigner and Kirkwood has also been calculated [22]. In a paper by Yang, corrections are derived in terms of the Green's function from the first-order reduced density matrix [15]. From these past works, it is well established that the ETF gradient corrections to TF, i.e., the gradient corrections for the slowly varying limit of a weakly perturbed uniform electron gas, are, to second order,

$$F_\tau^\mathrm{ETF}(s,q) = 1+\tfrac{5}{27}s^2+\tfrac{20}{9}q. \tag{8}$$

However, as explained in Sec. I, it has been observed that the ETF expansion does not apply universally to regions of slowly varying electron density in a system that is not a weakly perturbed uniform electron gas, but rather has surface regions, i.e., regions where the electron density drops to zero (see, e.g., Refs. [16] and [17]). The main idea put forward in this paper is to derive explicit corrections from a surface model system (the AG) and investigate how general the resulting expression is when applied to other model systems.

We note that the kinetic energy of the AG model and related systems has been discussed in other recent works. Vitos *et al.* [23] and Constantin and Ruzsinszky [24] have both presented KED functionals based on parametrizations of the AG KED. Both works discuss the role of the Laplacian term in achieving an optimal local description of the KED across the surface. Constantin and Ruzsinszky specifically enforce the ETF GE in the limit of slowly varying density. In contrast, in the present work, our focus is the exact behavior in the limit of slowly varying electron density far inside the surface.

Electronic edges and the AG

The derivations in the present work start from the formalism and results by Kohn and Mattsson [18], which are outlined in the following. We start from the general model system of an edge electron gas (EG) taken to be an inhomogeneous system of electrons with an *electronic edge*. The edge is defined in terms of the classical turning points

$$v_\mathrm{s}(\boldsymbol{r}) = \mu, \tag{9}$$

where v_s is the KS effective potential and μ is between the highest occupied and lowest unoccupied KS eigenvalue. This describes a surface (in the mathematical sense) outside of which the orbitals decay at an exponential rate. We take v_s to be constant in two spatial directions while varying in the third. The resulting KS orbitals are labeled with the quantum numbers $\nu=(k_1,k_2,\eta)$, where the k_i are plane-wave numbers for the x and y dimensions and η is the quantum number associated with the z dimension. Note that η can either be a continuous or discrete quantum number, depending on

the energy spectrum of the potential across the surface. In Ref. [18], the electron density of the EG for a general $v_s(z)$ is found to be

$$n^{\mathrm{EG}}(\boldsymbol{r}) = \frac{1}{\pi}\sum_{\eta:\epsilon_\eta \leqslant \mu} \varphi_\eta^2(z)|\mu - \epsilon_\eta|, \tag{10}$$

where $\{\varphi_\eta\}_{\eta=1}^{\infty}$ are the corresponding eigenfunctions in the z direction.

Furthermore, the AG is an edge gas with a linear potential,

$$v_s^{\mathrm{AG}}(\boldsymbol{r}) = \begin{cases} Fz, & z \geqslant -L \\ +\infty & \text{otherwise,} \end{cases} \tag{11}$$

where $F > 0$ is the slope in the potential. This slope defines a characteristic length $l \equiv \sqrt[3]{\frac{1}{2F}}$. Apart from Ref. [18], similar models have also been investigated in a number of previous works [23–28]. The KS equation

$$\left(-\frac{1}{2}\frac{d^2}{dz^2} + Fz\right)\varphi_\eta = \epsilon_\eta \varphi_\eta(z), \tag{12}$$

with $\varphi_\eta(-L) = \varphi_\eta(\infty) = 0$, has the solutions

$$\varphi_\eta(z) = \frac{\sqrt{\pi}}{\sqrt[4]{Ll}}\mathrm{Ai}\left(\frac{z}{l} + \frac{\epsilon_\eta}{\epsilon}\right), \tag{13}$$

and eigenvalues

$$\epsilon_\eta = -\eta\sqrt{\frac{l}{L}}\pi\tilde{\epsilon}, \quad \text{with} \quad \tilde{\epsilon} \equiv \sqrt[3]{\frac{F^2}{2}}, \tag{14}$$

where Ai are Airy functions. The orbitals and eigenvalues scale directly with l, which makes the AG effectively a zero parameter model. The absolute energy scale is chosen to make the chemical potential equal to zero. The eigenvalues $\{\epsilon_\eta\}_{\eta=1}^{\infty}$ are equally spaced and form a countable set. We introduce the scaled coordinate and scaled eigenvalues as, respectively,

$$\zeta \equiv z/l, \quad \epsilon \equiv \epsilon_\eta/\tilde{\epsilon}. \tag{15}$$

As we take the limit $L \to \infty$, the eigenvalues turn into a continuous eigenspectrum, i.e.,

$$\frac{\Delta\epsilon_\eta}{\tilde{\epsilon}} \to d\epsilon \Rightarrow \sum_{\epsilon_\eta}\frac{\Delta\epsilon_\eta}{\tilde{\epsilon}} \to \int d\epsilon. \tag{16}$$

Using Eqs. (13) and (16) in Eq. (10) gives the AG electron density,

$$n_0^{\mathrm{AG}}(\zeta) = \frac{1}{2\pi}\int_0^\infty d\epsilon\epsilon\,\mathrm{Ai}^2(\zeta - \epsilon), \tag{17}$$

with $n^{\mathrm{AG}}(z/l) = (1/l^3)n_0^{\mathrm{AG}}(\zeta)$. By Eq. (A.4) in Ref. [29], we then have

$$n_0^{\mathrm{AG}}(\zeta) = \frac{1}{6\pi}\left[2\zeta^2\mathrm{Ai}^2(\zeta) - \mathrm{Ai}(\zeta)\mathrm{Ai}'(\zeta) - 2\zeta\mathrm{Ai}'^2(\zeta)\right]. \tag{18}$$

Successive differentiation with respect to ζ gives, for the dimensionless scaled gradient and Laplacian, respectively,

$$s^{\mathrm{AG}}(\zeta) = \frac{1}{2\pi}\frac{\mathrm{Ai}'^2(\zeta) - \zeta\mathrm{Ai}^2(\zeta)}{2(3\pi^2)^{1/3}\left[n_0^{\mathrm{AG}}(\zeta)\right]^{4/3}}, \tag{19}$$

$$q^{\mathrm{AG}}(\zeta) = \frac{1}{2\pi}\frac{\mathrm{Ai}^2(\zeta)}{4(3\pi^2)^{2/3}\left[n_0^{\mathrm{AG}}(\zeta)\right]^{5/3}}, \tag{20}$$

where we note that $\zeta \to -\infty \Rightarrow s,q \to 0$, which means that the far inner region of the AG is a limit of slowly varying density. However, this limit of slowly varying density is fundamentally different from that in a weakly perturbed uniform electron gas.

III. THE KED IN THE AIRY GAS

In this section, we derive the central result of this work: a GE based on the AG model system, i.e., a GE up to second order in s and q that includes the quantum corrections due to the surface. Starting from the definition of the positive KED in Eq. (3) and using Eq. (10) gives

$$\tau^{\mathrm{EG}}(z) = \frac{1}{2}\sum_{\eta:\epsilon_\eta \leqslant \mu}\left[\frac{|\mu - \epsilon_\eta|^2}{2\pi}\varphi_\eta^2(z) + \frac{|\mu - \epsilon_\eta|}{2\pi}\varphi_\eta'^2(z)\right], \tag{21}$$

where we have used that the orbital energies satisfy $\frac{1}{2}(k_1^2 + k_2^2) + \epsilon_\eta \leqslant \mu$. Equation (21) is a general expression for the positive KED of an EG. As was previously mentioned, we take, for the AG, $\mu = 0$.

Inserting the AG orbitals of Eq. (13) into Eq. (21) and taking $L \to \infty$ results in an expression for the KED in terms of integrals over Ai functions,

$$\tau_0^{\mathrm{AG}}(\zeta) = \left\{\frac{1}{8\pi}\int_0^\infty d\epsilon\epsilon^2\mathrm{Ai}^2(\zeta - \epsilon) + \frac{1}{4\pi}\int_0^\infty d\epsilon\epsilon\left[\frac{d}{d\zeta}\mathrm{Ai}(\zeta - \epsilon)\right]^2\right\}, \tag{22}$$

where $\tau^{\mathrm{AG}}(z/l) = l^{-5}\tau_0^{\mathrm{AG}}(\zeta)$. Equation (22) has previously been derived in Refs. [23] and [24], but we take the extra step using Eqs. (A.6) and (A.7) found in Ref. [29], arriving at

$$\tau_0^{\mathrm{AG}}(\zeta) = \frac{1}{20\pi}[2(1-\zeta^3)\mathrm{Ai}^2(\zeta) + \zeta\,\mathrm{Ai}(\zeta)\mathrm{Ai}'(\zeta) + 2\zeta^2\mathrm{Ai}'(\zeta)]. \tag{23}$$

This is an exact expression of closed form valid throughout the AG system. We are interested in the quantum oscillations in the regime of slowly varying electron density, i.e., where $s,q \to 0$ far inside the classically allowed region of the system.

In this limit, both $n_0^{\mathrm{AG}}(\zeta)$ and $\tau_0^{\mathrm{AG}}(\zeta)$ are *unbounded* continuous functions. Moreover, $\tau^{\mathrm{TF}}[n_0^{\mathrm{AG}}]$ is continuous and the exact refinement factor,

$$F^{\mathrm{AG}}(\zeta) = \frac{\tau_0^{\mathrm{AG}}(\zeta)}{\tau^{\mathrm{TF}}\left[n_0^{\mathrm{AG}}\right]}, \tag{24}$$

is bounded and analytic as $\zeta \to -\infty$. Expanding Eq. (24) in a series around $\zeta = -\infty$ gives

$$F^{\mathrm{AG}}(\zeta) = 1 + \frac{5\left[5 + 6\sin\left(\frac{4}{3}\zeta^{\frac{3}{2}}\right)\right]}{48\zeta^3} - \frac{55}{192}\left(\frac{1}{\zeta}\right)^{\frac{9}{2}}\cos\left(\frac{4}{3}\zeta^{\frac{3}{2}}\right) + \mathcal{O}\left(\frac{1}{\zeta^5}\right). \quad (25)$$

This expansion has previously been derived by Baltin [26]. In that paper, however, the KED is given in terms of n, rather than in the coordinate ζ. We now proceed by expanding the scaled gradient $s^{\mathrm{AG}}(\zeta)$ and Laplacian $q^{\mathrm{AG}}(\zeta)$ in a Taylor series in the same way. This gives us

$$s^{\mathrm{AG}}(\zeta) = \frac{3}{4}\left(\frac{1}{\zeta}\right)^{\frac{1}{3}} - \frac{3\cos\left(\frac{4}{3}\zeta^{\frac{3}{2}}\right)}{16\zeta^3} + \mathcal{O}\left(\frac{1}{\zeta^{\frac{1}{9}}}\right) \quad (26)$$

and

$$q^{\mathrm{AG}}(\zeta) = \frac{3\left[1 + \sin\left(\frac{4}{3}\zeta^{\frac{3}{2}}\right)\right]}{16\zeta^3} - \frac{5}{128}\left(\frac{1}{\zeta}\right)^{\frac{9}{2}}\cos\left(\frac{4}{3}\zeta^{\frac{3}{2}}\right) + \mathcal{O}\left(\frac{1}{\zeta^6}\right), \quad (27)$$

respectively. We note that Eqs. (25) and (27), to leading order, both contain terms proportional to

$$\frac{1}{\zeta^3}\sin\left(\frac{4}{3}\zeta^{\frac{3}{2}}\right). \quad (28)$$

Hence, by identification, we can extract the coefficient for a term proportional to the scaled Laplacian $q_{\mathrm{AG}}(\zeta)$. We get, to leading order,

$$F^{\mathrm{AG}}(\zeta) = 1 + \frac{10}{3}q^{\mathrm{AG}}(\zeta) - \frac{5}{48}\frac{1}{\zeta^3}. \quad (29)$$

The leading term in Eq. (26) is nonoscillatory, and the expression can thus be inverted to give, to leading order in s,

$$\zeta^{\mathrm{AG}}(s) = \frac{1}{2}\left(\frac{9}{2s^2}\right)^{\frac{1}{3}}. \quad (30)$$

If we substitute Eq. (30) into Eq. (29), we finally obtain, to second order in $|\nabla n|$, the expression

$$F(s,q) = 1 - \tfrac{5}{27}s^2 + \tfrac{10}{3}q. \quad (31)$$

The derivation of Eq. (31) is based on the identification of terms between Eqs. (25)–(27), but is unique in the sense that no other expression with only linear dependence on s^2 and q (i.e., to second order in $|\nabla n|$) can exactly reproduce the oscillatory first-order term in Eq. (25). The result is a refinement function derived from the limit of slowly varying density far inside the surface from a linear potential, i.e., it is a GE that itself *includes* the quantum corrections from a surface. Note that the term proportional to s^2 in Eq. (31) has the same coefficient as the ETF GE given by Eq. (8), but differs in sign, whereas the term proportional to q is completely different. The expression is a main result of this paper, and we will refer to it as the AG-GE. We are not aware of prior works that address the system dependence of GEs with quantum corrections, so there is no *a priori* reason to expect this expression to be broadly applicable to a large set of systems with surfaces. Nevertheless, in the following, we will investigate the possible generality of this expression in regions of slowly varying electron density in other model systems. However, our first numerical investigation is the behavior of the ETF GE and the AG-GE for the actual AG model system itself.

In Figs. 1(a) and 1(b), we compare numerically the exact AG KED, the AG-GE, and the ETF GE far inside the inner region of the AG, and across the surface region. We see that the correction provided by Eq. (31) over ETF is crucial to properly account for the oscillations in the KED far from the surface. In the edge region, both of the expansions are expected to fail, since in this region the density is not slowly varying. However, it appears that the quantum corrections included in Eq. (31) worsen the result in this region compared to ETF.

IV. NUMERICAL RESULTS

In the following sections, we will explore the validity of Eq. (31) in comparison with the ETF GE for a number of model systems. We stress that these model systems are to be understood formally as giving model densities, which follows from the fact that the exact solution for a given KS potential is known. Consequently, no iteration for self-consistency is involved; we simply take the exact density of the model system and insert it into the respective expressions.

A. Jellium surface model

We turn first to the jellium surface model system [30]. The jellium surface under consideration has a value of the Wigner-Seitz radius $r_s = \{3/[4\pi n(\boldsymbol{r})]\}^{1/3}$ equal to 2. The numerically calculated exact refinement factor is shown together with both of the GEs in Figs. 1(c) and 1(d) far inside the surface where $s,q \to 0$, and across the surface region. The results are very similar to Figs. 1(a) and 1(b) for the AG. We see how the KED is accurately described by the AG-GE in Eq. (31) in the region of slowly varying electron density, while the ETF GE produces oscillations with a slightly too low amplitude. As we discussed for the AG, here also the ETF GE reproduces the exact behavior better across the surface region, whereas the AG-GE deviates more as we leave the region of slowly varying electron density. The results shown in Figs. 1(c) and 1(d) are also representative for other values that we investigated in the range 2 to 4 of the Wigner-Seitz radius. This is expected due to the scaling behavior of the KED.

B. Isotropic harmonic oscillator

Next we consider a model system that is very different from the AG and jellium surface: the isotropic (radially symmetric) harmonic oscillator (HO) in three dimensions. This model system contains a finite number of N electrons. The potential is

$$v_{\mathrm{s}}^{\mathrm{HO}}(r) = \tfrac{1}{2}\omega^2 r^2, \quad (32)$$

where ω is the angular frequency and r is the radial distance from the position of equilibrium. We let $\eta = 0,1,\ldots$ be the collective principal quantum number of the three oscillating modes and introduce the curvature parameter $w = \omega/2$. At

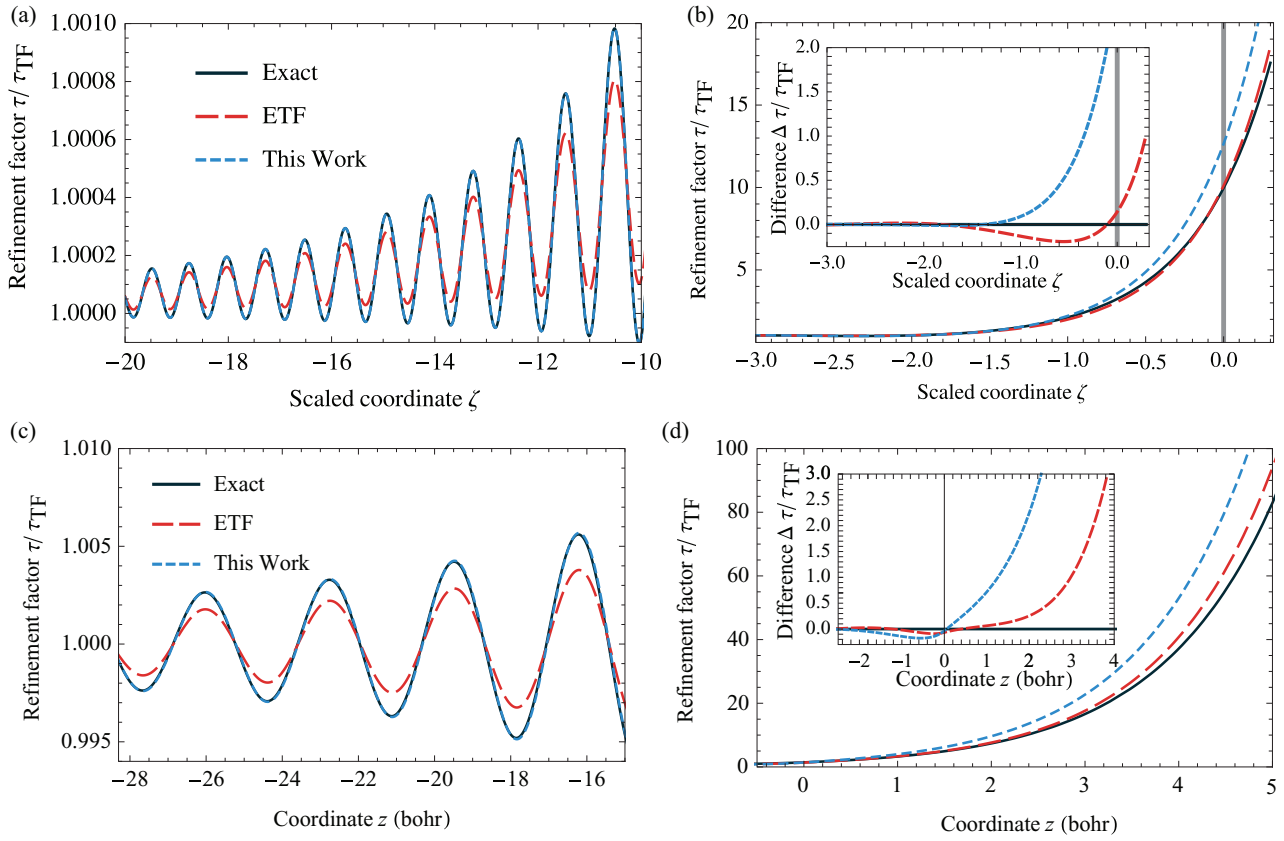

FIG. 1. (Color online) The ETF GE and the AG-GE in Eq. (31) compared to the exact KED for (a), (b) the AG and (c), (d) a jellium surface with $r_s = 2$. The AG system shown in (a) and (b) is the system used to derive the AG-GE. These panels are placed side by side with the corresponding application of the expressions in (c), (d) the jellium system for comparison. (a) The behavior far inside the AG surface ($\zeta \to -\infty$) as a function of the scaled coordinate ζ. The GE derived from the AG unsurprisingly describes the oscillations in the KED well, whereas the ETF GE does not. (b) The behavior in the surface region of the AG. The vertical line shows the position of the classical turning point. The inset shows the difference between the two expansions and the exact KED. (c) The regime of slowly varying electron density at large negative z of the jellium model. Also for the jellium system, the AG-GE describes the oscillations in the KED well, whereas the ETF GE fails to do so. This closely mimics the behavior seen for the AG in (a). (d) The surface region of the jellium model. In both (b) and (d), the ETF GE deviates less than the AG-GE from the exact KED over the surface region.

curvature ω, the first $(\eta + 1)$th energy levels are filled, where

$$\eta = \left\lfloor \frac{1}{2w} - \frac{3}{2} \right\rfloor. \tag{33}$$

Hence, systems with smaller w, which is a wider potential, contain more electrons.

Figures 2(a) and 2(b) show a HO system filled up to the 30th energy level, both close to the center (where the density is slowly varying) and across the surface. Despite the fact that the isotropic HO is a closed finite system, the results are surprisingly similar to the open AG and jellium models shown in Fig. 1. In the regime where the electron density is slowly varying, i.e., where s and q are relatively small, the oscillations reproduced by the ETF are too small in amplitude, but they are well reproduced by the AG-GE in Eq. (31). On the other hand, across the surface, the ETF more closely follows the exact KED, for this finite system also.

The study in Fig. 2 is of a specific highly filled HO system such that the electron density is sufficiently slowly varying. However, to truly realize the *limit* of slowly varying electron density in this system requires taking the curvature parameter $w \to 0$. Hence, in Fig. 3(a), we have selected one arbitrary spatial point in the system, $r_0 = 0.2$, and show the behavior of both GEs as $w \to 0$. This study confirms the foregoing conclusions: the AG-GE in Eq. (31) shows a strongly convergent trend, whereas the ETF appear consistently inaccurate as $w \to 0$.

As an aside on the topic of the KE in the HO model, we remark that the KE and electron densities of the harmonic oscillator in arbitrary dimensions d have been thoroughly investigated by Brack and van Zyl [31]. In their paper, they show that the TF KED, i.e., $\tau^{TF}[n]$, locally is a good approximant to the exact kinetic energy density for any value of d, but they do not discuss in detail the nature of the gradient corrections to the TF. Moreover, for $d = 2$, they verify that $\tau^{TF}[n]$ gives the exact total energy when integrated. It has been proven that TF densities are good approximations in the large particle-number limit $N \to \infty$ [32], and this fact has been demonstrated explicitly for the isotropic harmonic oscillator [33].

C. The Bohr atom

Another radially symmetric finite system of general interest is particles confined in a hydrogenlike potential, a model

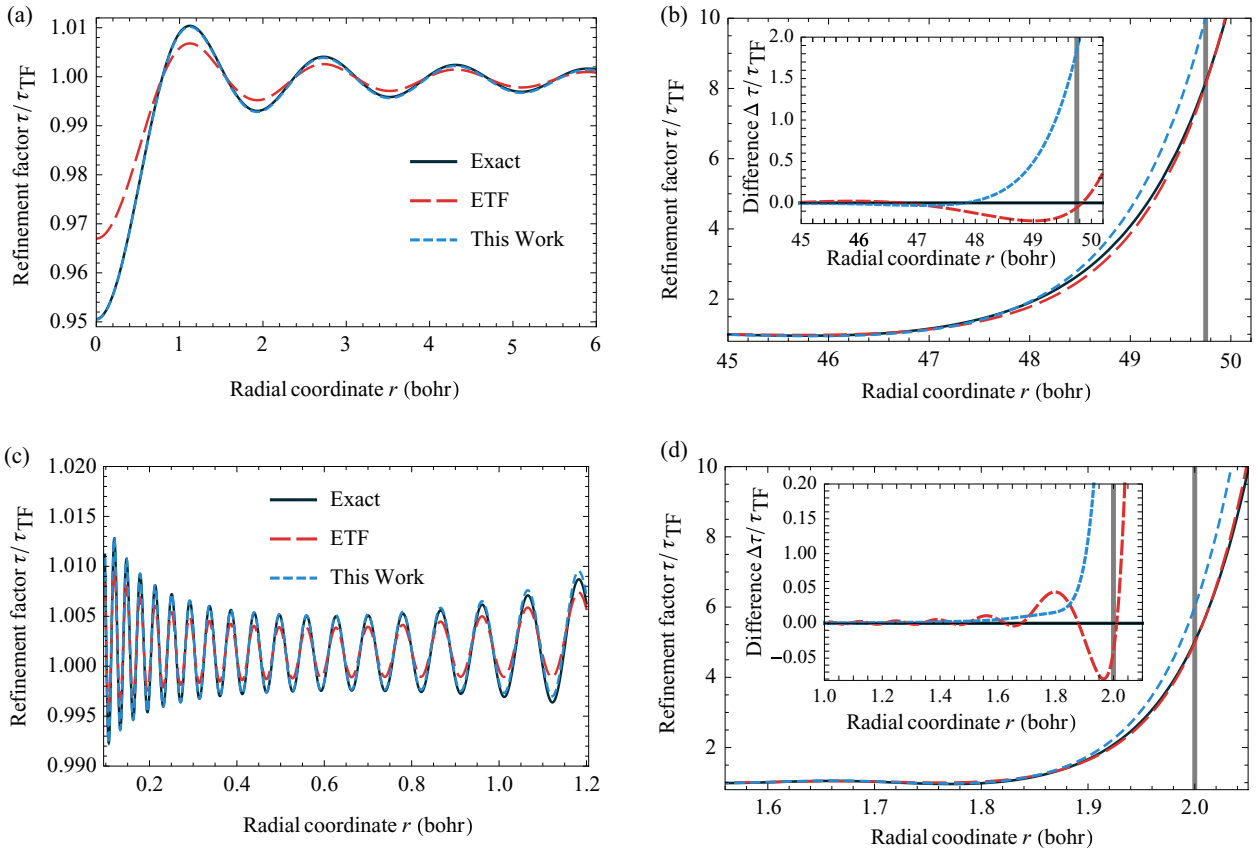

FIG. 2. (Color online) The ETF GE and the AG-GE in Eq. (31) compared to the exact KED for the (a), (b) isotropic harmonic oscillator and (c), (d) Bohr atom. Both systems show the same characteristics as were observed in Fig. 1. The AG-GE accurately describes the oscillations where the density is slowly varying, i.e., s and q are small [shown in (a) and (c)], whereas ETF fails to do so. However, across the edge [shown in (b) and (d)], the error in ETF GE is generally smaller than for the AG-GE.

system previously referred to as the Bohr atom [34]. The potential is

$$v_s^{\mathrm{HL}}(\boldsymbol{r}) = -\frac{Z}{|\boldsymbol{r}|}, \tag{34}$$

where Z is the atomic number. For any positive Z, this system has infinitely many bound states with eigenvalues

$$\epsilon_\eta = -\frac{Z^2}{2}\frac{1}{\eta^2}, \tag{35}$$

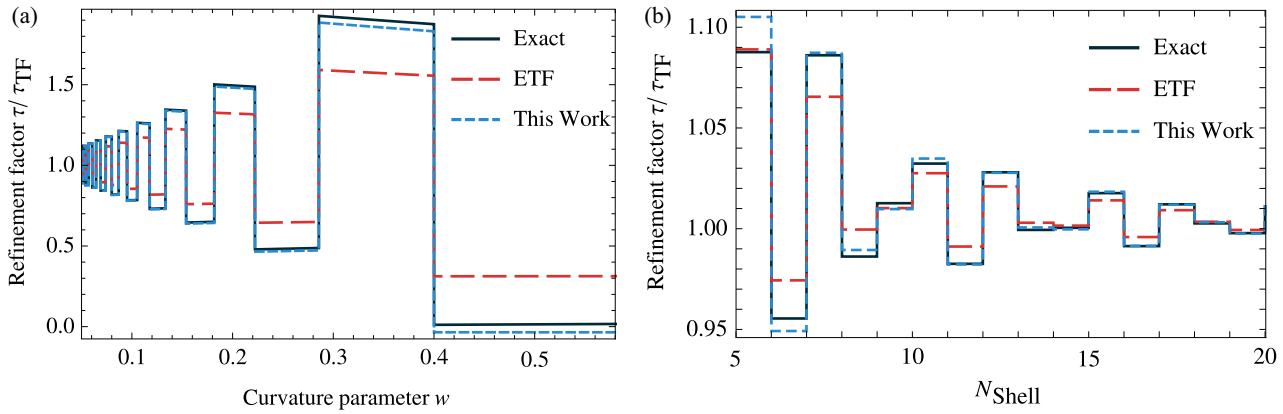

FIG. 3. (Color online) Convergence of the ETF GE and the AG-GE in Eq. (31) in an arbitrarily chosen single point for the (a) isotropic HO and (b) Bohr atom. (a) The isotropic HO at $r_0 = 0.2$ for the curvature parameter $w \to 0$, i.e., as the system fills up with more particles. Even at moderate values of w, the AG-GE reproduces the exact KED with great accuracy, whereas the ETF GE does not. (b) The Bohr atom at the arbitrarily chosen point $r_0 = 0.5$ as the number of filled shells N_{shell} increases. Similar to (a), the AG-GE accurately reproduces the KED in the limit of large N_{shell}, but the ETF GE does not.

where $\eta = 1,2,\ldots$ is the principal quantum number and there is an η^2-fold degeneracy in quantum numbers l and m. We take the system to be filled with particles up to $\eta = N_{\text{shell}}$, which means that it contains $N = 2\sum_{\eta=1}^{N_{\text{shell}}} \eta^2 = (1/3)N_{\text{shell}}(N_{\text{shell}}+1)(2N_{\text{shell}}+1)$ particles (including the spin degree of freedom). Note that the Z parameter just becomes a scaling factor in all expressions. Hence, the Bohr atom is effectively a one-parameter model. There is therefore no need to enforce $Z = N$ (i.e., the choice that would correspond to a neutral atom for interacting particles), and we can instead take $Z = N_{\text{shell}}^2$ to simplify the expressions without loss of generality. This makes the single parameter in this model N_{shell}. Appendix A1 give further details on this model, including the expression for τ.

Figures 2(c) and 2(d) shows a Bohr atom filled up to the 30th shell. In Fig. 2(c), the region where the electron density varies the least is pictured, i.e., where s and q are of smallest magnitude at an intermediate distance from the center. In Fig. 2(d), a region across the electronic surface of the atom is shown. The Bohr atom shares the same general behavior as the other models considered so far. In the region where the electron density is slowly varying (i.e., where s and q are relatively small), the oscillatory behavior is well described by the AG-GE in Eq. (31), whereas the ETF give oscillations with too small amplitude. Across the surface, we see how the ETF again follows the exact KED much more closely than the AG-GE. We also provide in Fig. 3 the behavior for the Bohr atom of the two GEs for one arbitrarily chosen spatial point in the system, i.e., $r_0 = 0.5$, as N is increased. This test further corroborates the conclusion of the convergence of the AG-GE in the limit of slowly varying density.

D. Mathieu gas

We now turn to a model system that, in contrast to the previous model systems, can model a weakly perturbed uniform electron gas. This model system is called the Mathieu gas (MG), and it has been investigated in detail in Ref. [35]. The potential is taken to be periodic in the z dimension,

$$v_{\text{s}}^{\text{MG}}(\boldsymbol{r}) = \lambda(1 - \cos(pz)), \tag{36}$$

where λ is the amplitude and p is the wave vector assigned to the oscillation. We introduce the scaled parameters

$$\bar{\lambda} = \frac{\lambda}{\mu}, \quad \bar{p} = \frac{p}{2k_{\text{F}}}, \quad \text{and} \quad \bar{z} = k_{\text{F}}z, \tag{37}$$

where $k_{\text{F}} = \sqrt{2\mu}$ is the Fermi wave vector of the uniform electron gas, taken in the semiclassical limit as independent of position. Depending on the choice of $\bar{\lambda}$ and $\bar{p}$, the chemical potential μ will be above or below the maximums of v_{s}, i.e., the MG can be made to represent either a perturbed uniform electron gas or a system with an infinite number of classically forbidden regions. For further details on the properties relevant to this work, see Appendix B.

This model system has a two-dimensional parameter space set by the unitless numbers $\bar{\lambda}$ and $\bar{p}$. When $\bar{\lambda} \to 0$, we approach the free-electron gas, and when $\bar{\lambda} \to \infty$, the occupied energy levels in the z direction reach those of an Hermite gas (HG); see Sec. IV E. The parameter space is shown in Fig. 4. Any sequence of MG systems that approaches the origin of this plot ($\sqrt{2\bar{\lambda}\bar{p}^2} \to 0$ and $\bar{p} \to 0$) represents a possible limit of slowly varying density. There are infinitely many sequences of this kind. A path with $\bar{\lambda} > 1/2$ means the chemical potential stays below the maximum of the potential, and the system will have classically forbidden regions repeated periodically along the z axis. A path with $\bar{\lambda} < 1/2$ means the chemical potential stays above the maximums of the potential, and the system approaches a slowly varying limit along a path that resembles a perturbed uniform electron gas. The path with exactly the border value $\bar{\lambda} = 1/2$ represents systems where the chemical potential exactly tangents the maximums of the potential. This path is indicated by a solid line of Fig. 4 and splits the entire parameter space into two distinct regions, which we will refer to as the HG regime (values of $\bar{\lambda} > 1/2$) and the free-electron (FE) regime (values of $\bar{\lambda} < 1/2$).

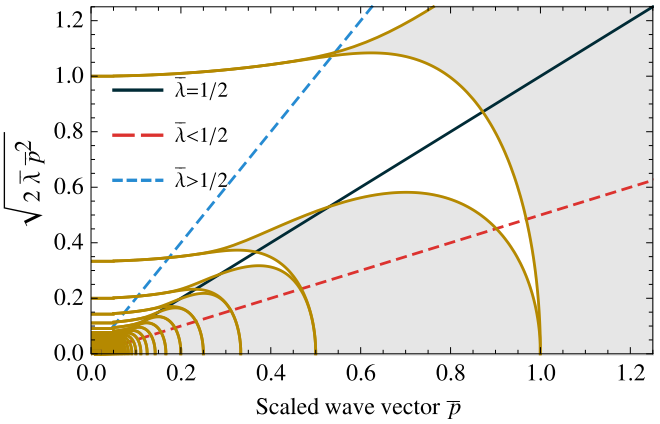

FIG. 4. (Color online) The parameter space of the Mathieu gas. The shaded area is defined by values of the chemical potential μ that belong to one of the possible energy bands of the energy spectrum in the z dimension. The light area is defined by values of the chemical potential μ in the FE continuum in x and y between the bands. Yellow lines correspond to values of the chemical potential situated precisely on the band edges of the energy spectrum in the z dimension. The straight lines in the parameter space correspond to different paths along which one can approach the limit of slowly varying electron density in the MG. The black line splits the parameter space into two distinct regions. The blue dashed line indicates a path to the limit of slowly varying density for which $\bar{\lambda} < 1/2$, and the red dashed line indicates a path to the limit of slowly varying density for which $\bar{\lambda} > 1/2$.

Our numerical investigation focuses on three different MG systems. The first MG system has $\bar{\lambda} = 0.1$ and $\bar{p} = 0.02$. This MG is in the FE regime of the parameter space, i.e., the system has no classical turning points. In Figs. 5(a) and 5(b), we show the KED of this system compared to the ETF GE and the AG-GE as a function of the scaled coordinate $\bar{z}$. As should be expected for a system which essentially is a straightforward realization of a weakly perturbed uniform electron gas, the ETF GE describes the KED well. On the other hand, the AG-GE clearly fails to reproduce the KED and appears shifted down even in the region near $\bar{z} = 0$, i.e., the region near the potential minimum where the values of s and q are the smallest.

Next we consider an MG with $\bar{\lambda} = 0.5$ and $\bar{p} = 0.015$, i.e., μ is precisely on the intersecting line between the HG and the FE regime. In this system, μ precisely tangents the maximums of the cosine potential. The result is shown in Figs. 5(c)

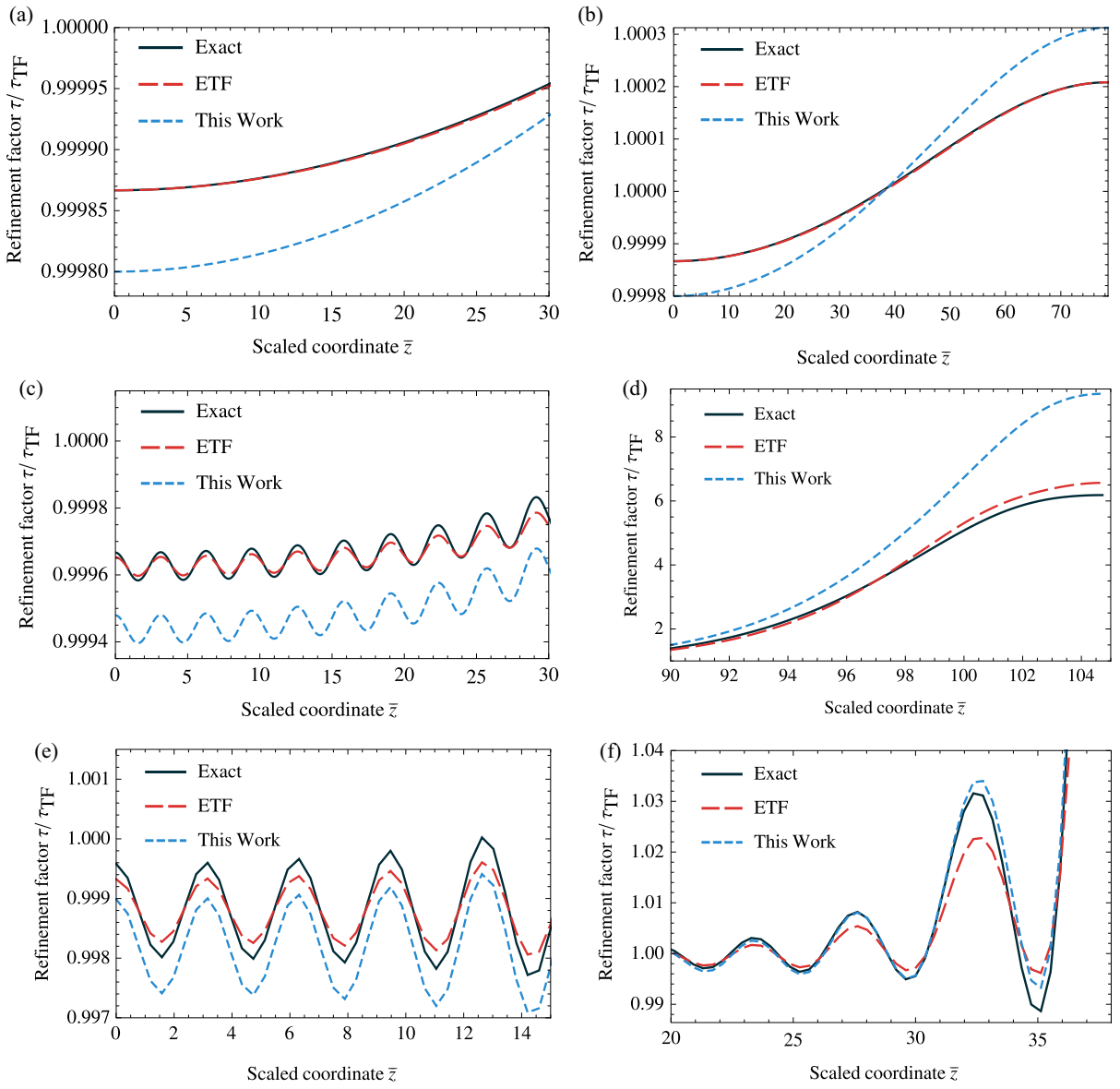

FIG. 5. (Color online) The ETF GE and the AG-GE in Eq. (31) compared to the exact KED for three different MG systems as a function of scaled spatial coordinate $\bar{z}$. (a), (b) The MG with $\bar{\lambda} = 0.1$, $\bar{p} = 0.02$, which has no forbidden regions and thus is FE-like. The ETF GE accurately describes the KED, whereas the AG-GE fails to do so. (c), (d) The MG with $\bar{\lambda} = 0.5$, $\bar{p} = 0.015$. In this MG, the chemical potential tangents the top of the potential. The ETF GE describes the system fairly well, but there appears to be a minor discrepancy in the amplitude of the oscillations. The AG-GE gives a description that is severely downshifted as compared to the exact KED. (e), (f) The MG with $\bar{\lambda} = 0.9$, $\bar{p} = 0.02$, where the chemical potential is far below the maximum values of the cosine potential, i.e., a system with an infinite number of classically forbidden regions. Both the ETF GE and AG-GE have oscillations that are similar to the exact KED. However, the oscillations in ETF appear to be of too small amplitude, whereas the AG-GE is shifted down relative to the exact KED.

and 5(d). In Fig. 5(c), oscillations have started to form because surfacelike behavior starts to manifest even before there are strictly classically forbidden regions—it is sufficient with regions where the potential maximums are close to the chemical potential. The ETF GE captures these oscillations but there is a visible discrepancy in the amplitude of the oscillations prevalent throughout the system. The AG-GE also displays the oscillations, but with a downwards shift compared to the exact KED. Figure 5(d) shows the surfacelike region of this MG. By periodicity, these regions repeat throughout the entire system. Similar to the other model systems studied above, the ETF appear to better reproduce the behavior in this region.

We finally consider the MG with an amplitude $\bar{\lambda} = 0.9$ and $\bar{p} = 0.02$. Here, μ is far below the maximums of the cosine potential. The exact KED is compared to the ETF GE and the AG-GE in Figs. 5(e) and 5(f). The general features are similar to the $\bar{\lambda} = 0.5$ case, but more clear here. Both of the GEs display oscillations similar to those in the exact KED. The ETF GE appears to underestimate the amplitude, whereas the AG-GE is shifted down. In absolute numbers, the incorrect offset of the AG-GE increases along the sequence of systems

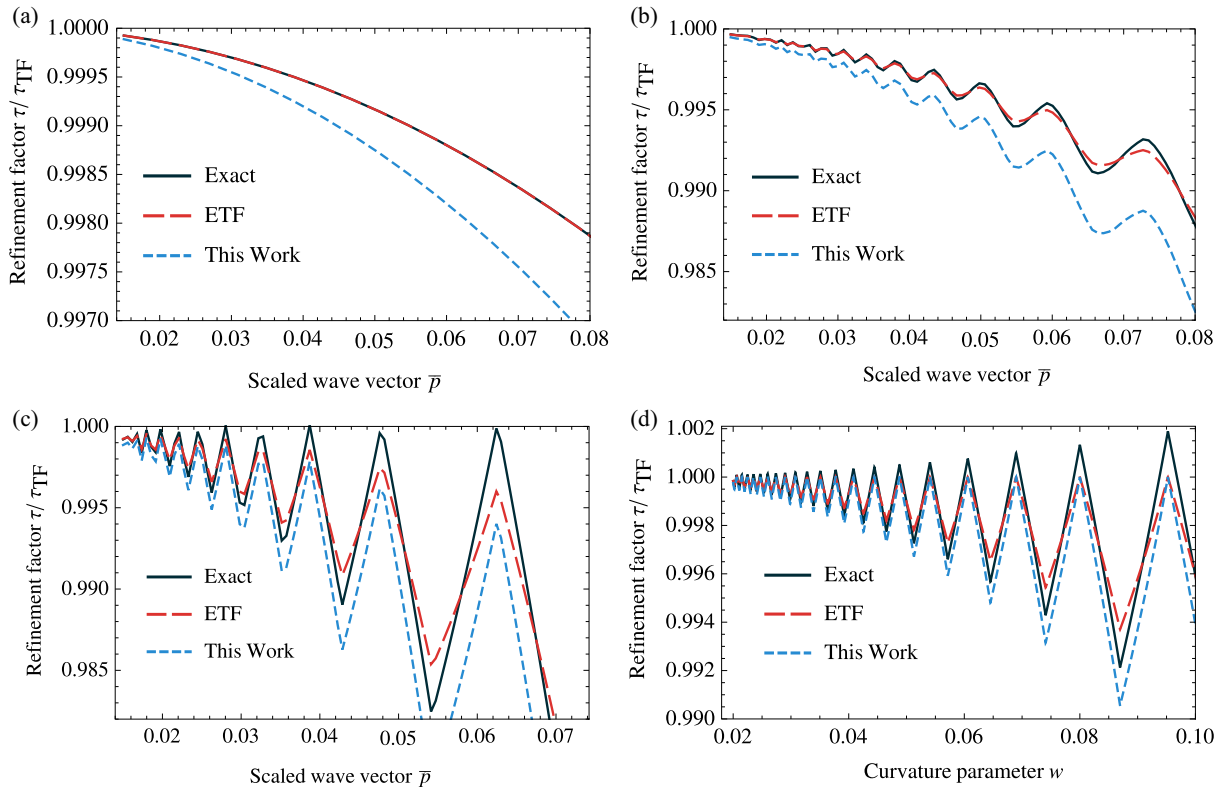

FIG. 6. (Color online) Convergence of the ETF GE and the AG-GE in Eq. (31) in one single arbitrarily chosen spatial point for MG systems ($\bar{z} = 0.01$) with (a)–(c) different parameters and (d) in the HG for $\bar{z} = 0$. (a) The convergence as the scaled wave vector $\bar{p}$ approaches zero for a MG with $\bar{\lambda} = 0.1$. In this MG, there are no classical turning points and the ETF GE appears to reproduce the exact KED well, whereas the AG-GE generally fails. (b) A MG with $\bar{\lambda} = 0.5$ for which the chemical potential tangents the top of the potential. (c) A MG with $\bar{\lambda} = 0.9$ where the chemical potential is far below the maximum values of the cosine potential, i.e., a system with an infinite number of classical turning points. Both the ETF GE and the AG-GE have oscillations that are similar to the exact KED in (b) and (c). However, the oscillations in ETF are of too small amplitude, whereas the AG-GE appears to be shifted down. (d) The HG in the limit of a curvature parameter $w \to 0$. The general behavior in the MG with large $\bar{\lambda}$ in (c) and the HG in (d) are very similar.

with increasing amplitude $\bar{\lambda}$, shown in Figs. 5(a), 5(c), and 5(e). However, relative to the size of the oscillations that appear in the systems, the offset becomes smaller.

We now move on to compare the convergence between the ETF GE and the AG-GE for one single arbitrary spatial point of the MG. For the three different MG systems with the rescaled amplitudes $\bar{\lambda} = 0.1$, $\bar{\lambda} = 0.5$, and $\bar{\lambda} = 0.9$, we will study the behavior in the arbitrarily chosen spatial point at scaled coordinate $\bar{z} = 0.01$. We let the scaled wave vector $\bar{p}$ approach zero, which takes us in a limit of a slowly varying density, $s,q \to 0$. The result is shown in Fig. 6. In Fig. 6(a), the MG with $\bar{\lambda} = 0.1$ is shown. As $\bar{p} \to 0$, the ETF GE moves closer to the exact KED, whereas the AG-GE consistently is too low. Figure 6(b) shows the convergence when $\bar{\lambda} = 0.5$. Now, the KED curve has visible oscillations. Then, as we approach the high-amplitude limit with $\bar{\lambda} = 0.9$, we see in Fig. 6(c) how the oscillations become sharper. Figures 6(b) and 6(c) confirm the same conclusions as were found in Fig. 5: neither the AG-GE nor the ETF appear to describe the limit of slowly varying density in MG model systems with large values of $\bar{\lambda}$ well. The ETF reproduces the oscillations with too small amplitude, and Eq. (31) is generally shifted down with respect to the exact KED.

E. Hermite gas

Since, in the previous section, we identified an issue with describing the KED of the MG in the large amplitude regime i.e., $\bar{\lambda} > 1/2$, we will now study a model system that represents the extreme case of $\bar{\lambda} \to \infty$. This limit is an EG with a harmonic oscillator potential, i.e., the Hermite gas (HG) discussed in Refs. [35] and [36]. The potential is

$$v_s^{\mathrm{HG}}(z) = \frac{\omega^2}{2} z^2, \tag{38}$$

where ω is the angular frequency of the oscillation and z is the distance from the equilibrium. The normalized eigenfunctions in the z direction are proportional to Hermite polynomials. The scaled parameters in this case are

$$w = \frac{\omega}{\mu}, \quad N(\mu) = \left\lfloor \frac{1}{w} - \frac{1}{2} \right\rfloor, \quad \bar{z} = k_{\mathrm{F}} z, \tag{39}$$

where $k_{\mathrm{F}} = \sqrt{2\mu}$, μ is the chemical potential, and $N(\mu)$ is the number of occupied orbitals in the z direction that is directly linked to the *curvature parameter* w which sets the curvature, and thus the width, of the potential parabola. Hence, the HG is effectively a one-parameter model. See Ref. [36] for additional properties of the HG. Further details regarding the HG relevant to this work can be found in Appendix C. The

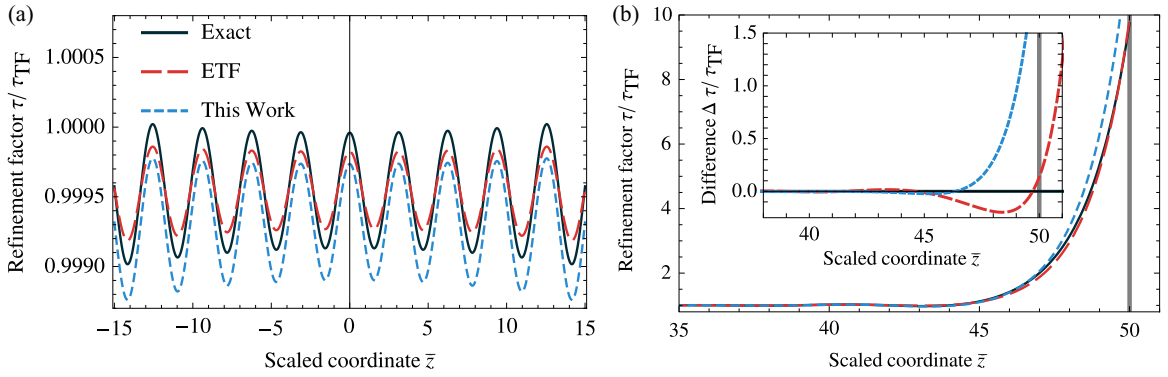

FIG. 7. (Color online) The HG filled up to the 30th energy level in the z-dimension energy spectra. (a) The exact KED for this system compared to the ETF GE and the AG-GE in Eq. (31) as a function of the scaled coordinate $\bar{z}$. The ETF GE underestimates the amplitude of the exact oscillation, whereas the AG-GE has a relative offset compared to the amplitude. (b) The surface region of the same system, where the vertical line is the classical turning point. The AG-GE has larger errors than the ETF GE in this surface region.

limit of slowly varying density is reached for $w \to 0$, which opens the harmonic potential to infinite width, while keeping the chemical potential constant.

We note briefly that the HG system expressions can be rescaled to give a different, but equivalent, view. The curvature w can be taken as fixed and the single parameter can be taken as μ. The limit of slowly varying density is then realized in a fixed energy spectra of the HG, with the levels filling up as $\mu \to \infty$.

We now study a HG filled with electrons up to the 30th energy level in the z direction. We are interested first in the classically allowed region. Figure 7(a) shows the exact KED for this system far away from the classical turning points compared to the ETF GE and the AG-GE in Eq. (31) as functions of the scaled coordinate $\bar{z}$. Similar to our observations for the large $\bar{\lambda}$ region of the MG model, we find that the ETF GE consistently underestimates the amplitude of the oscillations of the KED. On the other hand, Eq. (31) reproduces the amplitude well, but is shifted down compared to the exact KED. The surface region of this system is shown in Fig. 7(b). The ETF GE and the AG-GE both closely follow the exact KED in this region, but Eq. (31) deviates more than ETF near the classical turning point. In Fig. 6(d), convergence at the chosen point $\bar{z} = 0$ is shown. The tendency of the ETF GE to underestimate the amplitude of the oscillation and the relative offset of the AG-GE is seen here as well.

F. Comparison with other AG-based functionals

As was previously mentioned, the linear potential model system has been studied in several works. An early notable effort by Baltin [25,26] investigated the limits $s \to 0$ and $s \to \infty$, respectively, after obtaining the KED essentially by eliminating the potential and its gradient from the calculated first-order density matrix. Vitos *et al.* [23] performed a similar inversion but isolated a Laplacian term. We note that the functionals by Constantin and Ruzsinszky [24] are constructed to explicitly reproduce the ETF GE in s for the limit of a slowly varying density. They suggest that their $A_{1/6}$ functional will generally reproduce the surface data most accurately. These inversions are not, however, unique. They will all reproduce the exact KED specifically in the AG system, but will generally be different in other systems. The present work shows, however, that in the limit of slowly varying densities, the AG is locally exactly described by only one unique second-order GE. Figures 8(a) and 8(b) show the exact KED of a jellium surface for which $r_s = 1$, together with the AG-GE of Eq. (31) and the functionals proposed by Baltin and by Vitos *et al.* and the $A_{1/6}$ functional of Constantin and Ruzsinszky, respectively, for both the far inner region and across the surface region. The figure shows Eq. (14) of Vitos *et al.*, as Eq. (16) in their work behaves nonanalytically due to repeated singularities stemming from the zeros in the second-order derivative of the density. It is seen in Fig. 8(a) that the precise limit of the slowly varying density of only the jellium surface is accurately reproduced by Eq. (31), which means that none of the functionals reproduce the same GE in the limit of slowly varying electron density.

G. Total kinetic energies

Having discussed the performance of Eq. (31) as a semilocal approximation of the positive KED for edge systems, we now consider integrated values, i.e., total energies. The AG-GE is, by construction, only valid in the limit of a slowly varying density. We stress again that our aim in this work has been to investigate the exact behavior in this limit, not to develop an approximation that can be applied throughout a complete system with a surface region. An approximate expression that targets the whole system would clearly need to handle evanescent regions differently as compared to how the approximation was derived in the limit of a slowly varying density. For this reason, integrated values using Eq. (31) are expected to be outperformed by the ETF-GE because of the larger deviation from the exact KED we consistently see across the surface regions. The values of the integrated KEs are shown in Table I. The AG and jellium surface are completely open systems, infinite in size, and have therefore been omitted. In Table II, a comparison of the relative errors in the integrated KE values for the model systems is presented. To obtain numerical results, we used $F = 1/2$ and $l = 1$, but the relative error is independent of these values. Similarly, for the HG, we take the value $\mu = 1/2$ so that $k_F = 1$. Finally, for the MG, we take $\mu = 1/2$ so that $k_F = 1$. As is revealed in the tables, the ETF yields generally better values when used over the entire system.

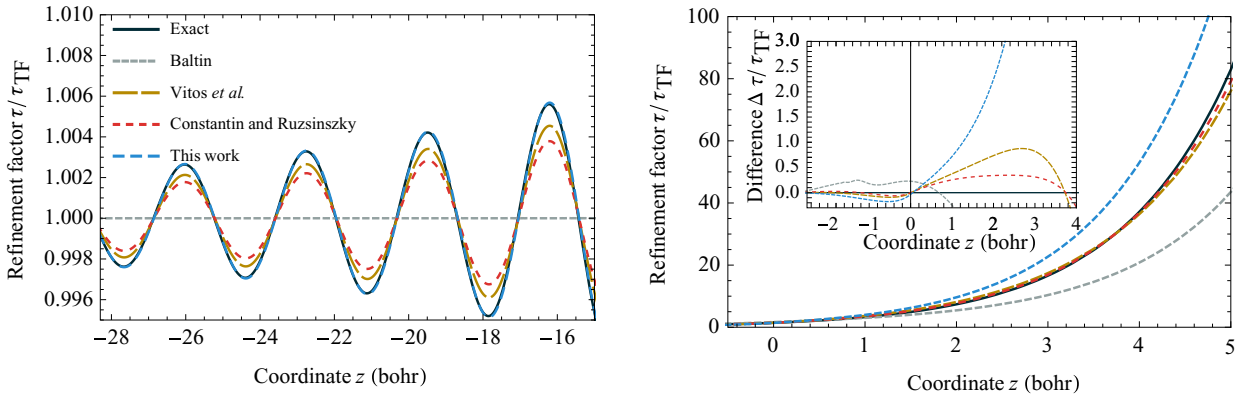

FIG. 8. (Color online) Exact KED for a jellium surface ($r_s = 1$) compared to the KEDs of other AG-based functionals (Baltin [25,26], Vitos *et al.* [23], and the $A_{1/6}$ functional of Constantin and Ruzsinszky [24]). (a) The limit of a slowly varying density. The expression by Baltin lacks a term proportional to the Laplacian and has oscillations of much less amplitude than the other functionals. The functional by Vitos *et al.* and the $A_{1/6}$ both somewhat underestimate the amplitude of the oscillations, whereas the AG-GE of Eq. (31) reproduces the amplitude correctly. (b) The surface region of the same system. The KED is well described by the functionals by Vitos *et al.* and Constantin and Ruzsinszky. The AG-GE and the expression by Baltin both significantly deviate from the exact KED in this region.

V. DISCUSSION

In this work, we have considered the influence of quantum oscillations due to electronic edges in the KED in the limit of slowly varying electron density. This has been achieved using the AG model system, which is a useful approximation of an inhomogeneous system of many electrons with a well-defined surface region [18]. Quantum oscillations in the KE and electron densities have previously been discussed [16,37] and they are known to not be captured by the ETF GE. On the other hand, the AG-GE in Eq. (31) is a gradient expansion that includes quantum gradient corrections from a linear surface. It is shown to describe the oscillations in the regime of slowly varying density in the jellium surface model and also in regions of slowly varying density in finite systems, i.e., the isotropic HO and the Bohr atom.

In surface regions, we observe from our numerical results that the ETF GE is generally more accurate than the AG-GE. This may seem surprising, given that the AG-GE is derived from a system that contains such a surface. The AG-GE and ETF GE are derived in very different ways, with the ETF GE based on a perturbed uniform electron gas, and the AG-GE as the extreme limit away from the surface. Hence, both GEs are far outside their formal domains of validity in the surface region. It appears that an exact description of the limit of the oscillatory behavior of the KED far away from a surface is different from correctly describing the physics across the surface. We have no further explanation as to why exactly the ETF GE appear to work better in this region. Furthermore, the AG-GE does not appear to represent the KED well in the limit of slowly varying density of the MG and HG model systems. In the low-amplitude regime (i.e., $\bar{\lambda} < 1/2$) of the MG, this is perfectly expected, since there is no classically forbidden region in the system, i.e., the system has no surface. For this case, the ETF GE is within its domain of validity throughout the system without any quantum oscillations. One may at a first think that the KED of the *high-amplitude* MG, and indeed the HG, should be well represented by the AG-GE, since these systems have surface regions. What is seen, however, is that none of the expansions reproduce well the KED in these systems.

The failure of both of the GEs for the MG and HG systems may be the result of system dependence of the quantum corrections in spite of the apparent generality of the AG-GE for other systems with surfaces. However, our results lead us to speculate that the behavior may rather be a consequence of the

TABLE I. Comparison of integrated total KE values for the model systems discussed in this paper. For the closed systems (HO and the Bohr atom), values are given in hartree. For the HG, values are given in hartree per unit area. For the MG, the values are given in hartree per unit area and per period. The AG and jellium surface give infinite total energies. For the parameters chosen for the MG, the absolute difference between ETF and AG-GE is smaller than can be seen in the significant digits shown here. See Table II for the relative error.

Model system	Exact refinement	ETF	AG-GE
Iso. HO	7.380×10^{3}	7.382×10^{3}	7.371×10^{3}
Bohr atom	2.430×10^{7}	2.428×10^{7}	2.408×10^{7}
$MG_{\bar{\lambda}=0.1}$	6.1857×10^{-1}	6.1857×10^{-1}	6.1857×10^{-1}
$MG_{\bar{\lambda}=0.5}$	3.6024×10^{-1}	3.6022×10^{-1}	3.6022×10^{-1}
$MG_{\bar{\lambda}=0.9}$	1.9276×10^{-1}	1.9277×10^{-1}	1.9263×10^{-1}
HG	2.4112	2.4112	2.4108

TABLE II. Comparison of relative errors in integrated total KE values for the model systems discussed in this paper.

Model system	ETF	AG-GE
AG	-7.2271×10^{-6}	2.0192×10^{-5}
Jellium ($r_s = 2$)	-3.7361×10^{-4}	-3.1099×10^{-3}
Iso. HO	1.9907×10^{-4}	-1.2840×10^{-3}
Bohr atom	-8.3199×10^{-4}	-9.1661×10^{-3}
$MG_{\bar{\lambda}=0.1}$	-1.1313×10^{-6}	-1.1322×10^{-6}
$MG_{\bar{\lambda}=0.5}$	-5.1908×10^{-5}	-6.0318×10^{-5}
$MG_{\bar{\lambda}=0.9}$	5.0042×10^{-5}	-6.7016×10^{-4}
HG	-1.8925×10^{-5}	-2.9987×10^{-4}

very strong anisotropy between the dimensions in the MG and HG systems. The energy levels in the AG are infinitely dense in all three dimensions. The two finite systems considered (the HO and the Bohr atom) are spherically symmetric and thus give a finite number of energy levels that are equally dense in all dimensions. However, the MG with large $\bar{\lambda}$ and the HG both have infinitely dense levels only in the x and y dimensions, whereas for the z dimension there is a discrete spectrum (HO) or a band structure (MG) where the bands get thinner as the potential amplitude $\bar{\lambda}$ increases. Our hypothesis thus means that the MG and HG systems may display a mix of both of the GEs. The ETF describes the changes in the KED as the chemical potential moves *between* two discrete energy levels in the z dimension, since such a change only adds plane-wave states in the x and y dimensions. On the other hand, as the chemical potential moves past the eigenvalues of states in the z dimension, the change in the KED is supposedly described well by the AG-GE. This would explain why the true behavior of the KED in these systems appears to share features of both GEs. However, if this interpretation is true, then the AG-GE may be of very broad general validity in describing quantum oscillations in systems with surface regions, as long as the systems do not have unreasonably anisotropic dimensions.

Development of kinetic energy functional $T_s[n]$

It is a long-term goal of functional development to construct viable approximations of the exchange-correlation and kinetic energy in DFT. Prior work on quantum corrections, as well as the present one, suggest that the electron density and KED in a classically allowed region where the electron density is slowly varying depend on the influence of nonlocal information, in the sense that the quantum oscillations are determined by the behavior of $v_s(\boldsymbol{r})$ outside the immediate neighborhood of the point $\boldsymbol{r}$. Surfaces and/or classical turning points are examples of such signatures in the topological landscape of the single-particle potential that influences the classically allowed region. The local energetics of the system in this region thus appears to differ between dissimilar systems and cannot uniquely be described in terms of a straightforward extension of TF theory solely by adding more terms in the local expansion (as is sometimes suggested, see, e.g., Ref. [38]).

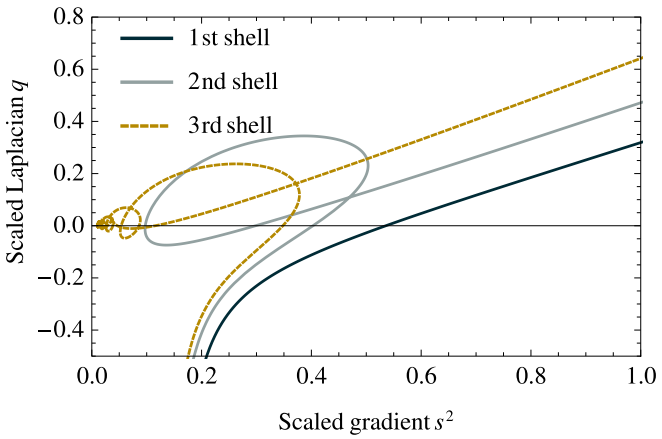

FIG. 9. (Color online) Contour plot that shows s^2 vs q over all values of r for the Bohr atoms filled up to and including the third shell. As the shell variable N_{shell} is increased, the number of loops increases and the curve approaches the origin, which demonstrates how the limit of slowly varying density is reached in this system within an intermediate region of r values.

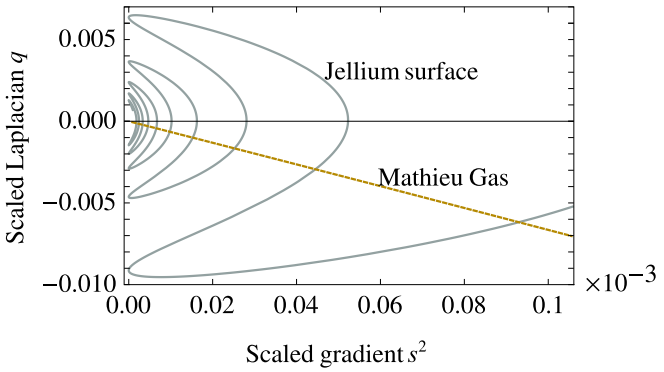

FIG. 10. (Color online) Contour plot of the scaled gradient s^2 vs the scaled Laplacian q in the limit of slowly varying density for the case of a jellium surface ($r_s = 1$) as $z \to -\infty$ and a Mathieu gas ($\bar{\lambda} = 0.1$) as $\bar{p} \to 0$.

One may at this point ask if a successful general semilocal approximation to τ valid for all limits of slowly varying electron density is even possible. Is it possible for such a semilocal approximation to differentiate between a situation where the ETF GE applies vs when the AG-GE applies, based only on the semilocal information available in $n(\boldsymbol{r})$, s, and q? To investigate this question, we look at the path in a contour plot of s^2 and q as we take the limit of slowly varying density in a few different model systems.

Two such contour plots are shown in Figs. 9 and 10. In Fig. 9, the behavior of the Bohr atom is shown to illustrate the complexity of how the limit of slowly varying density is achieved in these model systems. However, to address the question of the information available from s and q alone, we show in Fig. 10 both the jellium surface model and a low-amplitude MG overlaid into the same figure. We know that the limit of slowly varying density of the jellium surface model is accurately described by the AG-GE, whereas the ETF GE describes this particular low-amplitude MG very well. As is seen in the figure, the two systems approach the limit of slowly varying density very differently. However, there are points where the curves intersect and the local value of the two expansions are not the same in these points. This suggests that there cannot exist a simple semilocal approximation of $F(s,q)$ that gets both types of limits right. This appears to be a problematic conclusion in the development of approximative expressions. Nevertheless, it is possible that the precise difference between the AG-GE and the ETF GE this far into the limit of slowly varying electron density turns out to be energetically less relevant than other features of the KED.

VI. SUMMARY AND CONCLUSIONS

We have studied the AG in the limit far from the surface where the electron density is slowly varying. The presence of a surface region in the system (i.e., where the density decays to zero) requires quantum corrections compared to the usual

ETF GE. We have derived an expression for a GE incorporating such quantum corrections from the AG, i.e., the AG-GE, and find it to describe systems of both finite and infinite size with surface regions well. However, neither ETF nor the AG-GE appear to apply directly to the two model systems considered where the energy-level spacing is very anisotropic between different dimensions. Furthermore, while the present work has exclusively discussed the kinetic energy density τ, we now make a brief speculative remark on the possible relation of our findings to a different topic, i.e., the exchange energy density. The gradient coefficient in the GE for the exchange energy has been the subject of some debate, with Kleinman and Lee [39] arriving at the presently accepted value of 10/81 for a partially integrated GE that avoids a Laplacian term. The physics in the exchange term should be expected to be fundamentally different from the KE due to, e.g., the contributions from Coulomb interaction and Pauli repulsion. However, the present findings for the KED still highlight as a question whether it is possible that more than one relevant local gradient expansion could also exist for exchange. However, the situation for a local GE of the exchange energy density is much less clear than for the KED. Two of us have, in previous works, found that even for the MG in the limit of a weakly perturbed uniform electron gas, no such local GE appear to exist [35,40].

ACKNOWLEDGMENTS

We acknowledge support from the Swedish Research Council (VR), Grant No. 621-2011-4249, as well as the Linnaeus Environment at Linköping on Nanoscale Functional Materials (LiLi-NFM) funded by VR. A.L. thanks Dr. Olle Hellman for valuable input on the presentation. Sandia National Laboratories is a multi-program laboratory managed and operated by Sandia Corporation, a wholly owned subsidiary of Lockheed Martin Corporation, for the U.S. Department of Energy's National Nuclear Security Administration under contract DE-AC04- 94AL85000.

APPENDIX A: SYSTEMS WITH RADIAL SYMMETRY

Consider N noninteracting fermions in the spherically symmetric potential $v_s(r)$. The separable solutions to $\hat{H}_s\phi_\nu = \epsilon_\nu\phi_\nu$ are

$$\phi_\nu = \phi_{nlm}(r,\theta,\phi) = R_{nl}(r)Y_{lm}(\theta,\phi), \tag{A1}$$

where each R_{nl} is a radial distribution function and Y_{lm} are spherical harmonics. We wish to calculate the positive kinetic energy density

$$\tau(r,\theta,\phi) = \sum_{nlm} |\nabla\phi_{nlm}|^2. \tag{A2}$$

To this end, we calculate the gradient $\nabla\phi_{nlm}$ using the product rule

$$\nabla\phi_{nlm} = \nabla R_{nl}Y_{lm} + R_{nl}r\nabla Y_{lm}, \tag{A3}$$

where $\boldsymbol{\Psi}_{lm} = r\nabla Y_{lm}$ is the vector spherical harmonics along the ϕ direction. The $\boldsymbol{\Psi}_{lm}$ obey Unsöld's theorem [41], i.e.,

$$\sum_{m=-l}^{l} |\boldsymbol{\Psi}_{lm}|^2 = \frac{1}{4\pi}(2l+1)(l+1)l, \tag{A4}$$

which mirrors the fact that spatial densities must be radially symmetric. In the same way, the Y_{lm}'s obey the well-known addition theorem, i.e.,

$$\sum_{m=-l}^{l} |Y_{lm}|^2 = \frac{1}{4\pi}(2l+1). \tag{A5}$$

Hence, we are left with the expression for the radial KED:

$$\tau^{\text{Radial}}(r) = \frac{1}{4\pi}\sum_{n=1}^{N}\sum_{l=0}^{n-1}(2l+1) \times\left\{\left[\frac{\partial}{\partial r}R_{nl}(r)\right]^2 + l(l+1)\left[\frac{R_{nl}(r)}{r}\right]^2\right\}. \tag{A6}$$

KED of the Bohr atom

Consider noninteracting electrons that are bound by a potential of a Bohr atom, i.e.,

$$v_s^{\text{HL}}(\boldsymbol{r}) = -\frac{Z}{|\boldsymbol{r}|}, \tag{A7}$$

where Z is the atomic number. The system consists of a finite number of N electrons and the KS orbitals are the familiar functions

$$\phi_{\eta lm}(r,\theta,\phi) = R_{\eta l}(r)Y_{lm}(\theta,\phi), \tag{A8}$$

where the $R_{\eta l}$'s are proportional to Laguerre polynomials and the Y_{lm}'s are the normalized spherical harmonics. The eigenvalues are

$$\epsilon_\eta = -\frac{Z^2}{2}\frac{1}{\eta^2}. \tag{A9}$$

We take the system to be filled with particles up to principal quantum number $\eta = N_{\text{shell}}$, which means that it contains $N = 2\sum_{\eta=1}^{N_{\text{shell}}}\eta^2 = (1/3)N_{\text{shell}}(N_{\text{shell}}+1)(2N_{\text{shell}}+1)$ particles (including the spin degree of freedom). Furthermore, as explained in the main text, the atomic number Z scales the system, so we set $Z = N_{\text{shell}}^2$ to simplify the problem. Using Eq. (A6), the positive KED τ becomes

$$\tau^{\text{HL}}(r) = \frac{1}{4\pi}\sum_{\eta=1}^{N_{\text{shell}}}\sum_{l=0}^{\eta-1}(2l+1)\left(\frac{2Z}{\eta}\right)^3\frac{(\eta-l-1)!}{2\eta[(\eta+l)!]} \times\left(\left\{\frac{\partial}{\partial r}\left[e^{-\frac{Zr}{\eta}}\left(\frac{2Zr}{\eta}\right)^l L_{\eta-l-1}^{2l+1}\left(\frac{2Zr}{\eta}\right)\right]\right\}^2 + l(l+1)\left[\frac{1}{r}e^{-\frac{Zr}{\eta}}\left(\frac{2Zr}{\eta}\right)^l L_{\eta-l-1}^{2l+1}\left(\frac{2Zr}{\eta}\right)\right]^2\right). \tag{A10}$$

APPENDIX B: PROPERTIES OF THE MATHIEU GAS

Given a potential which is constant in two spatial directions and varies along the third, e.g., z, according to

$$v_s^{\text{MG}}(z) = \lambda(1-\cos(pz)), \tag{B1}$$

where λ is the amplitude and p is the wave vector of the oscillation, the solutions to the corresponding eigenvalue

problem are of the form

$$\varphi_\eta^{\mathrm{MG}}(z) = \frac{1}{L_3}\left[ce_\eta\left(z,-\frac{1}{2}\frac{\bar\lambda}{\bar p^2}\right)+ise_\eta\left(z,-\frac{1}{2}\frac{\bar\lambda}{\bar p^2}\right)\right] = \frac{1}{L_3}e^{i\eta\bar p\bar z}\sum_{k\in\mathbb{Z}}c_{2k}^\eta e^{i2k\bar p\bar z}, \tag{B2}$$

where $\eta\bar p k_{\mathrm F}L_3 = 2\pi n_3$ ($n_3\in\mathbb{Z}$), and L_3 is the size of the system, measured in units of z. Here, the functions ce_η and se_η are the real even and odd Mathieu functions, respectively. We have introduced the scaled parameters

$$\bar\lambda = \frac{\lambda}{\mu},\quad \bar p = \frac{p}{2k_{\mathrm F}},\quad \bar z = k_{\mathrm F}z, \tag{B3}$$

where $k_F = \sqrt{2\mu}$ is the Fermi wave vector of the uniform electron gas. The c_{2k}^η are found from the relation

$$(2k+\eta)^2c_{2k}^\eta - \frac{\bar\lambda}{2\bar p}\left(c_{2k-2}^\eta + c_{2k+2}^\eta\right) = a\left(\eta,\frac{\bar\lambda}{2\bar p^2}\right)c_{2k}^\eta, \tag{B4}$$

and they are normalized according to

$$\sum_{k\in\mathbb{Z}}\left|c_{2k}^\eta\right|^2 = 1. \tag{B5}$$

The eigenvalue associated with the φ_η are

$$\frac{\epsilon_\eta}{\mu} = \bar\lambda + \bar p^2 a\left(\eta,\frac{\bar\lambda}{2\bar p^2}\right). \tag{B6}$$

Using relation (21), the positive kinetic energy density becomes

$$\frac{\tau^{\mathrm{MG}}(z)}{\tau_u} = \frac{5}{2}\bar p\int_0^{\eta_m}d\eta\left\{\frac{1}{2}(1-\bar p^2a_\eta-\bar\lambda)^2\times\left[ce_\eta^2(\bar p\bar z,\bar q)+se_\eta^2(\bar p\bar z,\bar q)\right]+\bar p^2(1-\bar p^2a_\eta-\bar\lambda)\times\left[ce_\eta'^2(\bar p\bar z,\bar q)+se_\eta'^2(\bar p\bar z,\bar q)\right]\right\}, \tag{B7}$$

where $\tau_u = k_{\mathrm F}^5/(10\pi^2)$ and a_η are the eigenvalues of Eq. (B6), η_m is the energy of the highest occupied state, and $\bar q = -(1/2)\bar\lambda/\bar p^2$.

APPENDIX C: KED OF THE HERMITE GAS

For the HG, the potential varies along the z axis as an HO, i.e.,

$$v_{\mathrm s}^{\mathrm{HG}}(z) = \frac{\omega^2}{2}z^2. \tag{C1}$$

The eigenfunctions are the familiar

$$\varphi_\eta^{\mathrm{HG}}(z) = \left(\sqrt{\frac{\omega}{\pi}}\frac{1}{2^\eta\eta!}\right)^{1/2}H_\eta(\sqrt{\omega}z)e^{-\frac{\omega z^2}{2}}, \tag{C2}$$

with corresponding eigenvalues

$$\epsilon_\eta = \omega\left(\eta+\tfrac{1}{2}\right), \tag{C3}$$

for $\eta = 0,1,\ldots$. We introduce the scaled parameters,

$$w = \frac{\omega}{\mu},\quad N(\mu) = \left\lfloor\frac{1}{w}-\frac{1}{2}\right\rfloor,\quad \bar z = k_{\mathrm F}z, \tag{C4}$$

where $k_{\mathrm F} = \sqrt{2\mu}$, and $N(\mu)$ is the number of occupied z orbitals, respectively. Division with the KED of the free-electron gas yields the dimensionless quantity

$$\frac{\tau^{\mathrm{HG}}(\bar z)}{\tau_u} = \frac{1}{4\pi}\sqrt{\frac{w}{2\pi}}\sum_{\eta=0}^{N(\mu)}\frac{1}{2^\eta\eta!}\left[1-w\left(\eta+\frac{1}{2}\right)\right]\times\left\{\frac{1}{2}H_\eta^2\left(\sqrt{\frac{w}{2}}\bar z\right)e^{-\frac{1}{2}w\bar z^2}\left[1-w\left(\eta+\frac{1}{2}\right)\right]+\left\{\frac{d}{d\bar z}\left[H_\eta\left(\sqrt{\frac{w}{2}}\bar z\right)e^{-\frac{w\bar z^2}{4}}\right]\right\}^2\right\}. \tag{C5}$$

Note that the *curvature parameter* w describing the wideness of the potential parabola now directly determines the number of occupied orbitals in the z direction.

[1] P. Hohenberg and W. Kohn, Phys. Rev. **136**, B864 (1964).
[2] W. Kohn and L. J. Sham, Phys. Rev. **140**, A1133 (1965).
[3] R. M. Dreizler and E. K. U. Gross, *Density Functional Theory* (Springer, Berlin, 1990).
[4] V. V. Karasiev, D. Chakraborty, and S. B. Trickey, *Progress on New Approaches to Old Ideas: Orbital-free Density Functionals* in *Many-Electron Approaches in Physics, Chemistry and Mathematics: A Multidisciplinary View*, edited by L. Delle Site and V. Bach (Springer, Berlin, 2013).
[5] Y. A. Wang, N. Govind, and E. A. Carter, Phys. Rev. B **60**, 16350 (1999).
[6] J. P. Perdew and L. A. Constantin, Phys. Rev. B **75**, 155109 (2007).
[7] D. Lee, L. A. Constantin, J. P. Perdew, and K. Burke, J. Chem. Phys. **130**, 034107 (2009).
[8] I. Z. Petkov and M. V. Stoitsov, *Nuclear Density Functional Theory* (Oxford University Press, New York, 1991).
[9] K. M. Daily, D. Rakshit, and D. Blume, Phys. Rev. Lett. **109**, 030401 (2012).
[10] L. H. Thomas, Proc. Cambridge Philos. Soc. **23**, 542 (1927).
[11] E. Fermi, Z. Phys. **73** (1928).
[12] D. A. Kirzhnits, Sov. Phys. JETP **5**, 64 (1957).
[13] C. H. Hodges, Can. J. Phys. **51**, 1428 (1973).
[14] M. Brack, B. K. Jennings, and Y. H. Chu, Phys. Lett. B **65**, 1 (1976).
[15] W. Yang, Phys. Rev. A **34**, 4575 (1986).
[16] W. Kohn and L. J. Sham, Phys. Rev. **137**, A1697 (1965).
[17] P. Elliott, D. Lee, A. Cangi, and K. Burke, Phys. Rev. Lett. **100**, 256406 (2008).
[18] W. Kohn and A. E. Mattsson, Phys. Rev. Lett. **81**, 3487 (1998).

[19] E. Engel and R. M. Dreizler, *Density Functional Theory* (Springer, Berlin, 2011).
[20] R. G. Parr and W. Yang, *Density-Functional Theory of Atoms and Molecules* (Oxford University Press, New York, 1989).
[21] C. F. V. Weizsäcker, Z. Phys. **96** (1935).
[22] B. K. Jennings and R. K. Bhaduri, Nucl. Phys. A **253**, 29 (1975).
[23] L. Vitos, B. Johansson, J. Kollár, and H. L. Skriver, Phys. Rev. A **61**, 052511 (2000).
[24] L. A. Constantin and A. Ruzsinszky, Phys. Rev. B **79**, 115117 (2009).
[25] R. Baltin, Phys. Lett. A **37**, 67 (1971).
[26] R. Baltin, Naturforsch. A **27**, 1176 (1972).
[27] A. G. Eguiluz, M. Heinrichsmeier, A. Fleszar, and W. Hanke, Phys. Rev. Lett. **68**, 1359 (1992).
[28] V. Sahni and A. Solomatin, Ann. Phys. **259**, 97 (1997).
[29] J. R. Albright, J. Phys. A: Math. Gen. **10**, 485 (1977).
[30] N. D. Lang and W. Kohn, Phys. Rev. B **1**, 4555 (1970).
[31] M. Brack and B. P. van Zyl, Phys. Rev. Lett. **86**, 1574 (2001).
[32] E. H. Lieb and B. Simon, Phys. Rev. Lett. **31**, 681 (1973).
[33] M. Brack and M. V. N. Murthy, J. Phys. A: Math. Gen. **36**, 1111 (2003).
[34] O. J. Heilmann and E. H. Lieb, Phys. Rev. A **52**, 3628 (1995).
[35] R. Armiento and A. E. Mattsson, Phys. Rev. B **66**, 165117 (2002).
[36] F. Hao, R. Armiento, and A. E. Mattsson, Phys. Rev. B **82**, 115103 (2010).
[37] M. A. Thorpe and D. J. Thouless, Nucl. Phys. A **156**, 225 (1970).
[38] E. W. Pearson and R. G. Gordon, J. Chem. Phys **82**, 881 (1985).
[39] L. Kleinman and S. Lee, Phys. Rev. B **37**, 4634 (1988).
[40] R. Armiento and A. E. Mattsson, Phys. Rev. B **68**, 245120 (2003).
[41] A. Unsöld, Ann. Phys. (Berlin) **82** (1927).